

## Hybrid functionalized phosphonate silica: insight into chromium removal chemistry from aqueous solutions

Pedro Iván Hernández-Velázquez<sup>1</sup>, José A. Gutiérrez-Ortega<sup>1</sup>, Gregorio Guadalupe Carbajal-Arizaga<sup>1</sup>, Ricardo Manríquez-González<sup>2</sup>, Wencel De la Cruz-Hernández<sup>3</sup>, Sergio Gómez-Salazar<sup>4\*</sup>

<sup>1</sup>Departamento de Química, Universidad de Guadalajara. Blvd. Marcelino García Barragán # 1421, esq. Calzada Olímpica, Guadalajara, Jalisco, México C.P. 44430.

<sup>2</sup>Departamento de Madera, Celulosa y Papel, Universidad de Guadalajara-CUCEI,. Km 15.5, carretera Guadalajara-Nogales, Las Agujas, Zapopan, Jalisco, México C.P. 45020.

<sup>3</sup>Centro de Nanociencias y Nanotecnología, Universidad Nacional Autónoma de México, km 107 carretera Tijuana-Ensenada, Ensenada, B.C. México C.P. 22830.

<sup>4</sup>Departamento de Ingeniería Química. Universidad de Guadalajara-CUCEI. Blvd. Marcelino García Barragán # 1421, esq. Calzada Olímpica, Guadalajara- CUCEI, Jalisco, México C.P. 44430.

\*Corresponding author: Sergio Gómez-Salazar, e-mail: [sergio.gomez@cucei.udg.mx](mailto:sergio.gomez@cucei.udg.mx). ORCID identifier is 0000-0002-3880-4632. Phone: +5533 1378 5900 Ext 27512

Received February 27<sup>th</sup>, 2019; Accepted May 20<sup>th</sup>, 2019.

DOI: <http://dx.doi.org/10.29356/jmcs.v63i2.793>

**Abstract.** Insight into Cr(III) ions removal chemistry from aqueous solutions was gained by using hybrid phosphonate-functionalized silica adsorbents synthesized through a modified route of sol-gel processing (SPMF). Evaluation of the degree of metal removal was obtained from kinetics and batch experiments. Elemental analysis, FTIR, NMR and XPS techniques were used to study the nature of surface complex formed on adsorbent. Adsorption equilibrium results showed a maximum Cr(III) removal of 78.639 mg g<sup>-1</sup> Cr(III) at pH 3.6 on adsorbent SPMF04; kinetics measurements indicated that equilibrium was reached in 80 min contact time. The achievement of 2.923 mmol P/g as phosphonate groups was obtained. A Langmuir-type mechanism explained the adsorption equilibrium results whereas kinetic measurements were explained through a pseudo-second order mechanism. FTIR measurements indicated a strong influence of Cr(III) adsorbed on surficial functional groups. <sup>29</sup>Si CP MAS NMR results indicated that Cr(III) interacted not only with phosphonate surface groups but also with a large amount of geminal OH surface groups. XPS studies suggested that Cr(III) was removed through the formation of the surface complex R as monovalent chromium acetate and/or divalent. The adsorbent SPMF04 can be potentially employed in industrial applications.

**Keywords:** amorphous silica; sol-gel process; Cr(III) ions; NMR; XPS.

**Resumen.** Información sobre la química de remoción de Cr(III) de soluciones acuosas fue obtenida usando adsorbentes de sílice híbrida funcionalizada con fosfonato sintetizados a través de una ruta modificada del proceso sol-gel (SPMF). La evaluación del grado de remoción de metal fue obtenida a partir de experimentos de cinética y por lotes. Técnicas de análisis elemental, FTIR, NMR y XPS fueron usadas para estudiar la naturaleza del complejo de superficie formado sobre el adsorbente. Los resultados del equilibrio de adsorción mostraron una remoción máxima de Cr(III) de 78.639 mg g<sup>-1</sup> Cr(III) a pH 3.6 sobre el adsorbente SPMF04; las mediciones cinéticas indicaron que el equilibrio fue alcanzado en 80 min de tiempo de contacto. El logro de 2.923 mmol P/g como grupos fosfonato fue obtenido. Un mecanismo tipo Langmuir explicó los resultados del equilibrio de adsorción mientras que las mediciones cinéticas fueron explicadas a través de un mecanismo de pseudo-segundo orden. Los resultados de <sup>29</sup>Si CP MAS NMR indicaron que Cr (III) interactuó no solamente con grupos fosfonato de superficie sino también con una gran cantidad de grupos OH de superficie

geminales. Los estudios de XPS sugirieron que Cr(III) fue removido a través de la formación del complejo de superficie R como acetato de cromo monovalente y/o divalente. El adsorbente SPMF04 puede ser potencialmente empleado en aplicaciones industriales.

**Palabras clave:** Silice amorfa; proceso sol-gel; iones Cr(III); NMR; XPS.

---

## Introduction

The removal of toxic metal ions from aqueous streams requires the use and implementation of new environment friendly materials. Due to its high toxicity [1], [2] and threat to public health and to the environment, chromium is set as of high priority for removal. In the environment, this metal is established as one of the most toxic metals [3]–[5]. In nature, chromium is present in two oxidation states, Cr(III) and Cr(VI). Cr(VI) shows more toxicity than Cr(III); it is carcinogenic and mutagenic. However, Cr(III) shows toxicity to plants at elevated concentrations and presents less toxicity to animals, but trace levels of this element affect sugar and lipid metabolism in humans. Despite the fact that Cr(III) presents less toxicity compared to Cr(VI), elevated levels can be present in the environment as a consequence of non-treated discharges or badly treated streams from industries or the disposal of chromium-containing sludges [6]–[11]. The World Health Organization (WHO) sets the maximum allowable concentration in drinking water for total Cr should be 0.05 mg/L [12], [13], whereas the United States Environmental Protection Agency (USEPA) sets the limit to 0.01 mg L<sup>-1</sup> [14].

Chromium-containing wastes come from industrial streams including electroplating, metal finishing, leather tanning, pigments, leather and wood preservation, and the manufacture of dyes and pigments [15]. Nowadays, industry is in search of replacing metal recovery and separation techniques thus conducting to the development of recovery techniques including: membrane separation, lime softening, electrodialysis, coagulation/filtration, the use of materials based on mineral [16], [17], biomass [18], and ion exchangers [19]. These techniques show a low capacity of metal extraction or metal removal slow kinetics. Ion exchangers present the drawback of fouling after several cycles of adsorption and desorption of metal and they also present fixed removal capacity. At present, diverse removal techniques have appeared in the literature in order to separate chromium ions from aqueous solutions. Amongst the most widely used methods are foam flotation and electrocoagulation. In the former one, metal removal process is applied based on the reaction between chromium ions and an oppositely charged ionic surface-active reagent (collecting surfactant) [20]. On the other hand, electrocoagulation [21-23] involves the generation of coagulants by dissolving metal electrodes or free electrons. The metal ions formed are metal hydroxides, like Al(OH)<sub>2</sub><sup>+</sup>, Al(OH)<sub>2</sub><sup>2+</sup>, and Al(OH)<sub>4</sub><sup>-</sup> for Al electrode, and Fe(OH)<sub>2</sub><sup>+</sup> and Fe(OH)<sub>3</sub> for Fe electrode. Therefore, there is the need to find new techniques and materials that could help in overcoming these limitations. Recently, a new type of materials based on the adsorption phenomenon has appeared. Different works on the removal of Cr (III) onto waste solids, like agrowaste biosorbents [24]–[26] and materials based on silica [27]–[29] were found in the literature.

In the last few years, chemically modified silica gel adsorbents have become attractive materials for the extraction of metal ions and different types of compounds, due to the fact that these materials do not swell, nor shrink, like in the case of polymeric resins. Moreover, the modified silica has both good thermal stability and high metal removal efficiency [30]; because of this new procedures to produce adsorbent materials have been developed, among which the ones that use hybrid and functionalized adsorbents via the sol-gel process [31], [32] is proposed. These adsorbents contain an inorganic matrix which can be silica, alumina, titania or zirconia, to which functional organic groups are adhered such as thiols, amine, phosphonates, carboxylates, halides, etc., which play the role of ligand agents for metal ions, metalloids, non-metal cations (like NH<sub>4</sub><sup>+</sup>) or of non-metal anions (like seleniate) [33]. The most used techniques to synthesize these materials include elimination or separation (deposition) of solvent, where a solvent is employed to attach the functional groups to the ceramic support by Van der Waals forces [34]. Another synthesis route is the covalent attachment which is based in hydrolysis and condensation reactions between the surface of the inorganic material and a hydrolysable reactant containing the desired functional group, thus obtaining coupling of functional groups

with ceramic matrix via non-hydrolysable covalent bonding [35]. However, with these techniques are obtained materials with a low adsorption capacity mainly due to a poor density of functional groups on the surface of adsorbent. Sol-gel process has demonstrated to be very efficient in the synthesis of hybrid adsorbents. This process consists in obtaining a sol and its gelation followed by solvent removal by evaporation [36]. Materials synthesized by this method are characterized by possessing high mechanical resistance, high densities of functional groups, excellent thermal and chemical stability, high adsorption capacities, good selectivity towards specific metals and it is possible to control their specific surface area, pore size and pore size distributions [37].

In this work, it is presented the synthesis of high-density phosphonate-functionalized mesoporous adsorbents by the sol-gel technique applied to chromium (III) removal from aqueous solutions. Due to our interest in applying the adsorbents to the industrial level, cross-linked adsorbents such as functionalized silica synthesized under soft reaction conditions, the sol-gel method was used to prepare phosphonate-functionalized materials with the expectation of having improved ligand densities, better chromium adsorption kinetics, and mesoporous arrangement so that the entrance of metal ions to surface active sites is favored. Hence, the aim of this work is to investigate on the properties of adsorbents applied into the removal chemistry of Cr(III) ions from aqueous streams. The obtained adsorbents were characterized by elemental analysis, N<sub>2</sub> adsorption measurements, solid-state <sup>13</sup>C, <sup>31</sup>P MAS, and <sup>29</sup>Si CPMAS NMR, and Fourier transform infrared (FTIR). The adsorption behavior of chromium ions onto adsorbents was studied in batch mode. Several kinetic models were applied in order to explain the experimental data of Cr(III) ion removal by adsorbents. X-ray photoelectron spectroscopy (XPS) was applied to study the chemical environment of chromium on the surface of materials and to propose a surface complex formed upon adsorption of chromium.

## Experimental

### Materials

Tetraethyl orthosilicate (TEOS), [(3-trihydroxysilyl)propyl]methyl sodium phosphonate (SPMF) and triethylamine (TEA) were obtained from Sigma Aldrich (St. Louis, MO). Ethanol, acetone, acetic, hydrochloric, nitric acids, nonahydrated chromium nitrate, Cr(NO<sub>3</sub>)<sub>3</sub>•9H<sub>2</sub>O, sodium acetate, and sodium chloride were acquired from Fermont (Monterrey, Mexico). All Chemicals were analytical reagent grade and used as received. To prepare the reacting sample and aqueous solutions, deionized water was used (18 MΩ•cm) (Barnstead, Chicago, Ill). The pH measurements were carried out with a Thermo Orion 4 Star model pH meter. A ContrAA 300 Analytik Jena instrument (Jena, Germany) was used to measure chromium concentrations.

### Synthesis of SPMF adsorbents

The cross-linking agent tetraethoxy silane (TEOS) was mixed with ethanol, NaCl and HCl (as catalyst). The mixture was stirred for several minutes to allow hydrolysis (reaction 2.21 in Fig. 1) and TEOS homocondensation (reaction 2.22 in Fig. 1). A mixture of SPMFS and HCl was prepared separately (SPMFS:HCl = 1:1.28) and stirred for several minutes to allow homocondensation (reaction 2.23 in Fig. 1) of SPMFS. Then, the two solutions were mixed at several co-condensation times (reaction 2.24 in Fig. 1); TEA was then added to induce gelation of the reacting mixture. The gel obtained was aged for 24 h at ambient temperature and dried at 70 °C for 36 h. The dried sample was then subjected to a hydrothermal process consisting of refluxing the sample using a 50/50 % volume water/acetone mixture at 55-60 °C for 12 h. Then, the solution was replaced by fresh acetone three times. Finally, the dried solid (SPMF) was ground and sieved to a mesh 120. This particle size guarantees minimization of external mass transfer resistances during metal uptake [27]. Different molar ratios were studied during the synthesis as well as different hydrolysis/condensation times aiming to obtain an improved metal uptake.

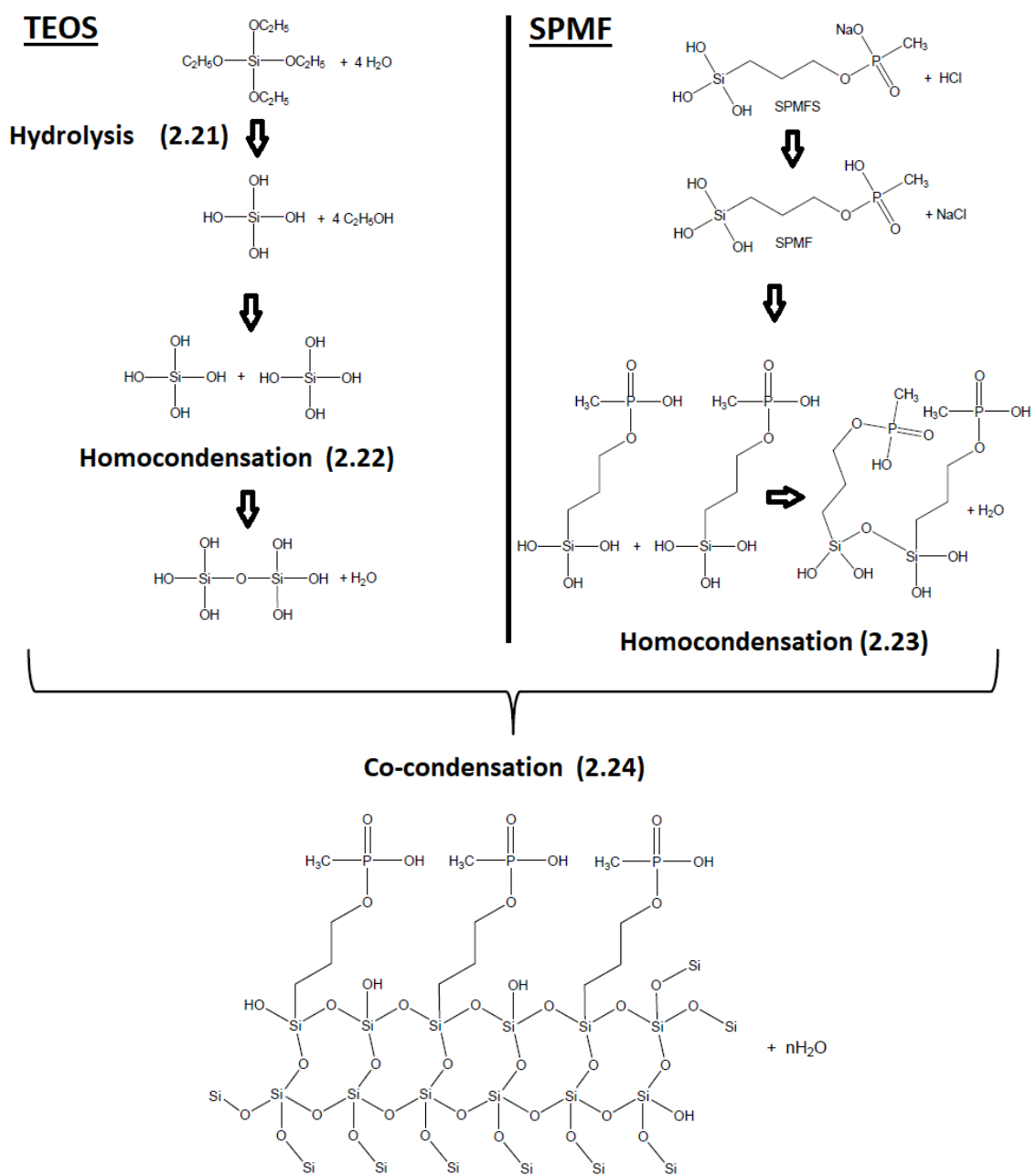


**Fig. 1.** Synthesis route used to prepare the SPMF adsorbents.

### Elemental analysis

These measurements were performed using a LECO TruSpec Micro instrument (St. Joseph, MI). About 2 mg of SPMF were used, heated at 1100°C and analyzed for C and the amount of phosphorus was determined indirectly by considering that for each gram of adsorbent, were obtained 8.42 mM of carbon and 2.11 mM of phosphorus. This ratio of 4:1 is in agreement with the equivalent amount of carbon/phosphorus (C/P) present in the propyl methyl phosphonate ligands. Every sample was analyzed in triplicate and averaged values reported.

### Nitrogen adsorption experiments

Nitrogen adsorption measurements were performed on an ASAP 2020 KMP (Micromeritics, Norcross, GA) instrument at 77 K. Approximately 1 g of sample was heated at 65°C for 8 h under vacuum to remove all impurities. The BET surface area ( $S_{BET}$ ) was calculated using the BET equation. Pore size, and pore size distributions were calculated using the BJH method [38].

### Adsorption kinetics of Cr(III)

These measurements were carried out to determine the time at which adsorbent SPMF04 reaches Cr(III) uptake equilibrium. Three metal concentrations were used: 400, 200 and 100 mg L<sup>-1</sup> Cr(III). A .05 M sodium acetate was used as buffer at pH of 3.60. About 0.2 g of adsorbent were contacted with 50 mL of initial Cr(III) ions in a thermostirrer (Thermo Fisher Scientific, Ohio, USA) at 120 rpm and 298 K and different times (0-300 min). Then, suspensions were filtered and concentrations of initial and final solutions of Cr(III) were measured by atomic absorption spectroscopy. The amount of Cr(III) adsorbed was obtained by a mass balance given by equation (1):

$$q = \frac{V(C_i - C_f)}{m} \quad (1)$$

where,  $q$  is the amount of Cr(III) adsorbed (mg g<sup>-1</sup>),  $C_i$  and  $C_f$  are the initial and final Cr(III) solution concentrations (mg L<sup>-1</sup>), respectively,  $V$  is the volume of solution (L),  $m$  is the mass of adsorbent (g). The equilibration time was considered as the one after which there was not a change in the amount of Cr(III) removed.

### Cr(III) adsorption equilibrium measurements

With the aim of finding the Cr(III) removal capacity and the effect on the adsorption of pH of solution by adsorbent SPMF04, adsorption equilibrium experiments were carried out at different pH's. Cr(III) solutions of varying concentrations (100 - 1200 mg L<sup>-1</sup>) were obtained in a pH range of 3 to 5.5. This pH range was selected because several industries discharge waters with heavy metals in this pH range. A 1500 mg L<sup>-1</sup> Cr(III) stock solution was prepared by dissolving 11.43 g of Cr(NO<sub>3</sub>)<sub>3</sub>·9H<sub>2</sub>O in 1000 mL of deionized water. Initial Cr(III) solutions were obtained from the stock solution by a dilution and 25 mL of a 0.5M sodium acetate were added for pH control. About 0.2 g of adsorbent SPMF04 were put in contact with 50 mL of initial Cr(III) solution in a thermostirrer (Thermo Fisher Scientific, Ohio, USA) at 120 rpm and 298 K for 3 h. After this, suspensions were filtered and initial and final amounts of Cr(III) in the solutions were measured by the atomic absorption technique. The amount of Cr(III) adsorbed was calculated by equation (1). Triplicate runs were performed and average values are used.

### Selectivity experiment

This experiment was conducted with the purpose of determining the affinity adsorbent SPMF04 presents toward a metal ion when is present in a multimetallic solution (Cr, Cd, Ni, Pb, Zn, Cu). For this experiment, a stock solution was prepared with equimolar concentrations of each cation (0.684 mmol). The amounts of each metal in this solution ion yield 20% saturation of the adsorbent. About 0.2g of adsorbent was put in contact with 50 mL of the multimetallic solution in a thermostirrer (Thermo Fisher Scientific, Ohio, USA) at 120 rpm and 298 K for 24 h. After this, suspensions were filtered; then the concentrations of initial and final solutions were measured for Cr, Cd, Cu, Zn, Pb and Ni. Each metal adsorbed (in mg/g) was obtained by equation (1). Triplicate runs were performed and average values are used.

### FTIR measurements

Functional groups identification on material SPMF04 and a general chemical characterization, was obtained from the FTIR measurements before and after Cr(III) removal by SPMF04. Measurements were conducted using a Perkin Elmer Spectrum One spectrometer employing the KBr waffle technique. A number of 50 scans were used in the range of 450-4000  $\text{cm}^{-1}$  with a resolution of 4  $\text{cm}^{-1}$ .

### NMR measurements

The NMR spectra of SPMF04 and SPMF04-Cr(III) samples in the solid state were obtained to evaluate the formation of: 1) the silicon matrix by  $^{29}\text{Si}$ , 2) the presence of the active organic part in the material by  $^{13}\text{C}$  and  $^{31}\text{P}$  and, 3) to study metal interactions by means of changes in the signal patterns of the material before and after Cr(III) uptake. The spectra were obtained employing an NMR Bruker spectrometer model Advance III 300 under a magnetic field of 7T, using a 4 mm probe head with a spinning speed of 8 kHz.  $^{13}\text{C}$  spectra were obtained by a CP-MAS experiment employing a contact time of 2 ms and a transmitter frequency of 75.5 MHz. The  $^{29}\text{Si}$ , and  $^{31}\text{P}$  analyses were performed by the high power decoupling pulse experiment (HPDEC MAS) under frequencies of 59.5 and 121.4 MHz, respectively.

### XPS studies

XPS measurements were conducted to investigate the chemical environment of atoms on the pristine sample SPMF04 and to determine the surface complex formed on sample SPMF04-Cr. XPS data were obtained by using an XPS PHI 548 system; the base pressure was lower than  $2 \times 10^{-8}$  torr. XPS data collections were obtained by using an X-ray source nonmonochromatic (Al-K $\alpha$ ); operation was set at 300 W (15 kV and 20 mA). Acquisition of high-resolution scans was obtained by adjusting the pass energy to 50 eV and the pass established at 0.2 eV. Once base line subtraction was done by the Shirley method, curve fitting was conducted using an algorithm of nonlinear least squares assuming Gaussian peak shape. The position of hidden peaks was determined with the software XPSPEAK41 and according to reports from the literature.

## Results and discussion

### Synthesis of SPMF adsorbents and elemental analysis results

**Synthesis of SPMF adsorbents.** In this work, different tests were conducted for the synthesis of adsorbents for Cr(III). These tests consisted of varying molar ratios of reactants as well as their reaction times (hydrolysis and condensation) in order to seek the adsorbents with the following characteristics: little solubility in water, high density of functional groups and improved metal uptake capacities. By the use of greater amounts of HCl during the synthesis process to the SPMFS mixture to lower the pH, formation of [(3-trihydroxysilyl)propyl]methyl phosphonate (SPMF) was achieved, which is more easy to manipulate and to homocondensate due to a lower reaction kinetics. Consequently, the materials SPMF01 through SPMF08 were synthesized by the complete sol-gel route as described earlier and by varying both molar ratios and reaction times (see table 1). The difference between these samples is the Condensación of SPMF and Co-condensation TEOS/SPMF reaction times. The eight adsorbents were then subjected to a maximum Cr(III) uptake test from a 3000 mg Cr(III)  $\text{L}^{-1}$  stock solution with 0.02 M acetate as buffer (see table 2). From this table, it can be seen that material SPMF04 was the one with the highest Cr(III) uptake (78.639  $\text{mg g}^{-1}$ ). These results are attributed to a greater density of functional groups (2.923  $\text{mmol P g}^{-1}$  from table 2) and to its increased surface area (1.0211  $\text{m}^2 \text{g}^{-1}$ ). It can be noticed that adsorbent SPMF06 has the highest density of functional groups (3.119  $\text{mmol P g}^{-1}$ ), however, due to the fact that this material has a lower specific surface area, the contact surface with Cr(III) decreases and is reflected in a lower uptake. In summary, mixture SPMF shows ease for its homocondensation while being previously hydrolyzed. However, the water content in which is dissolved the salt of SPMFS, prevents gelation of system with TEA in a way such that instead of obtaining precipitation of the system, a gelatin-like mixture is obtained after aging and drying processes, gelation of the system occurs as a first step followed by elimination of water, ethanol and TEA by evaporation and finally, the desired material is obtained.

**Table 1.** Molar ratios used in the synthesis of functionalized adsorbents with phosphonate groups.

| Material | Molar ratios |      |      |                  |       |              |      |                    | Time, min |                              |                   |                           |
|----------|--------------|------|------|------------------|-------|--------------|------|--------------------|-----------|------------------------------|-------------------|---------------------------|
|          | TEOS mixture |      |      |                  |       | SPMF mixture |      | Triethyl amine TEA | TEOS:SPMF | Hydrolysis/condensation TEOS | Condensation SPMF | Co-condensation TEOS/SPMF |
|          | TEOS         | EtOH | NaCl | H <sub>2</sub> O | HCl   | SPMF         | HCl  |                    |           |                              |                   |                           |
| SPMF01   | 1            | 4    | 0.01 | 4                | 0.006 | 1            | 1.28 | 0.12               | 1:1       | 15                           | 7                 | 7                         |
| SPMF02   | 1            | 4    | 0.01 | 4                | 0.006 | 1            | 1.28 | 0.12               | 1:1       | 15                           | 7                 | 15                        |
| SPMF03   | 1            | 4    | 0.01 | 4                | 0.006 | 1            | 1.28 | 0.12               | 1:1       | 15                           | 7                 | 30                        |
| SPMF04   | 1            | 4    | 0.01 | 4                | 0.006 | 1            | 1.28 | 0.12               | 1:1       | 15                           | 15                | 15                        |
| SPMF05   | 1            | 4    | 0.01 | 4                | 0.006 | 1            | 1.28 | 0.12               | 1:1       | 15                           | 30                | 15                        |
| SPMF06   | 1            | 4    | 0.01 | 4                | 0.006 | 1.5          | 1.92 | 0.13               | 1:1.5     | 15                           | 15                | 15                        |
| SPMF07   | 1            | 4    | 0.01 | 4                | 0.006 | 2            | 2.56 | 0.14               | 1:2       | 15                           | 15                | 15                        |
| SPMF08   | 1            | 4    | 0.01 | 4                | 0.006 | 3            | 3.84 | 0.14               | 1:3       | 15                           | 15                | 15                        |

**Table 2.** Densities of functional groups and maximum Cr(III) uptake on adsorbents SPMF.

| Material | mmol P/g     | q <sub>max</sub><br>(mg Cr(III) g <sup>-1</sup> ) |
|----------|--------------|---|
| SPMF-01  | 2.11 ± 0.073 | 37.4 ± 2.9  |
| SPMF-02  | 2.17 ± 0.134 | 44.1 ± 3.7  |
| SPMF-03  | 2.51 ± 0.168 | 66.9 ± 4.2  |
| SPMF-04  | 2.92 ± 0.078 | 78.6 ± 7.5  |
| SPMF-05  | 2.85 ± 0.229 | 56.7 ± 3.1  |
| SPMF-06  | 3.20 ± 0.181 | 61.3 ± 1.7  |
| SPMF-07  | 2.56 ± 0.269 | 61.1 ± 2.9  |
| SPMF-08  | 2.56 ± 0.089 | 49.7 ± 1.7  |

**Elemental analysis.** The results of these measurements are shown in table 2. It can be observed from this table that out of the first five adsorbents synthesized with a molar ratio of TEOS/SPMF 1:1, the material SMPF04 is the one that presents one the highest density of phosphorous (2.92 mmol P/g). It can also be observed from this table that the trend shown by these five adsorbents is similar to that of the maximum Cr(III) uptake (table 2). In this trend, an increase in the removal of Cr(III) is observed as well as in the concentration of functional groups from adsorbent SPMF01 through SPMF04 from which the trend decreases on adsorbent SPMF-05. These results suggest that the hydrolysis and condensation times are the appropriate to facilitate the greatest incorporation of functional groups to the silica net, as well as the formation of a greater surface area. In view of the results obtained from synthesis of adsorbents from elemental analysis, and maximum Cr(III) uptake, adsorbent SPMF04 was selected to be characterized by the different techniques to measure its physicochemical properties and the Cr(III) adsorption capacity.

### Nitrogen adsorption results

Despite the low surface area in this adsorbent (see supplementary material), a ligand density of  $2.92 \pm 0.078$  mmol P/g and  $q_{\max}$  of  $78.6 \pm 7.5$  mg Cr(III)  $g^{-1}$  was obtained. The low surface area can be explained by the fact that during synthesis of this adsorbent little branched particles were produced which tends to produce linear structures, since adsorbent was synthesized under acidic pH. In sol-gel processing the ultimate frame of the solid material is dependent on the aging and drying steps as well as on the catalyst used: it is known that the use of basic catalysts yield branched monoliths whereas acid catalysts yield poorly branched solids [39]. In addition, the growth of pores is commonly achieved by disintegration and condensation of the silica frame if alkaline solutions are employed for the aging of sol-gel monoliths [40]. In the synthesis of SPMF04, the aging step comprised a 50 v/v% water/acetone mixture heated to 60°C for 24 h. This mixture has a basic pH because of the presence of triethyl amine (TEA) used in the gelation of sol monoliths. The partition of silica portions from slim and obstructed pores on the surface of the solids will be accelerated by heating of adsorbent. A recombination of these partitioned silica portions will occur at the rounded section of the pores. However, structures formed from linear polymers possess the potential of having their ligand groups exposed since branched structures can have functional sites hidden or obstructed in the silica net thus limiting its metal uptake capacity. Finally, a type II isotherm is obtained (Fig. 2) and a slight H1 type hysteresis loop is observed according to the IUPAC designation, characteristic of aggregated samples (like silica gels) possessing poorly defined pore size distribution.

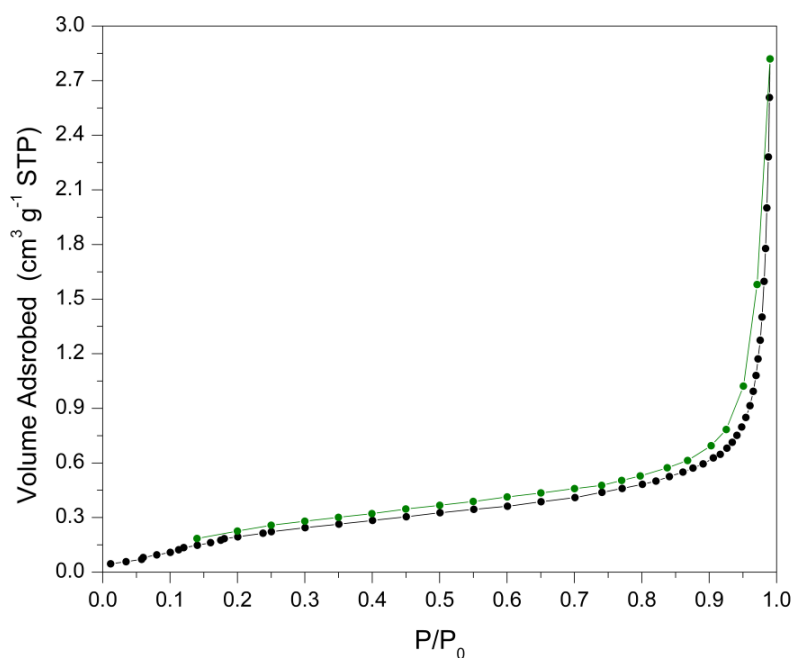
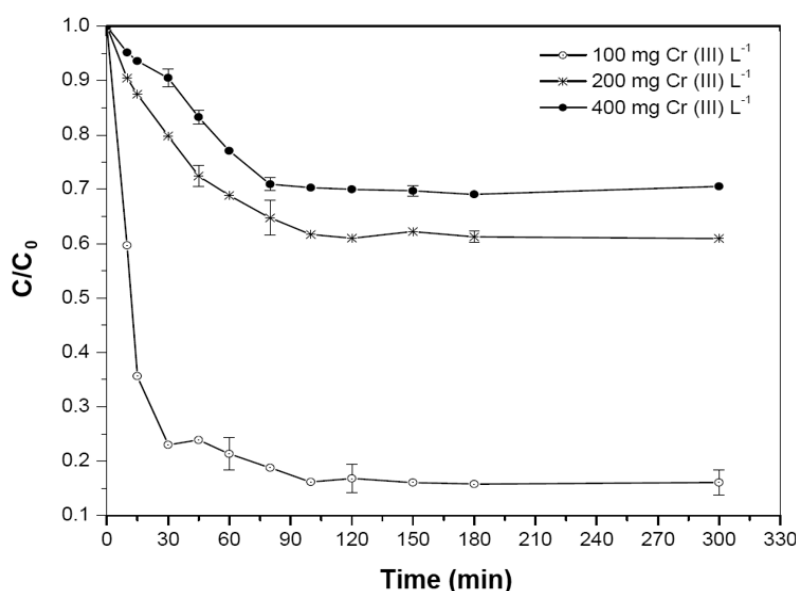


Fig. 2. Nitrogen adsorption isotherm on SPMF04 adsorbent at 77 K.

### Adsorption kinetics of Cr(III)

These measurements are useful in the determination of the time needed after which the system reaches adsorption equilibrium of Cr(III) ions. The kinetic results on adsorbent SPMF04 are shown in Fig. 3 for the three chromium concentrations analyzed (100, 200 and 400 mg Cr(III) L<sup>-1</sup>). It can be observed from this figure that from 80 min the adsorbent starts reaching adsorption equilibrium, thus showing low mass transfer resistances. The trends observed in the adsorption of Cr(III) gradually decrease with contact time, which can be due to reduction of availability in the amount of functional sites which are directly spaced. In addition, it can be observed from these experiments that adsorbent does not show a significant change in the adsorption equilibrium from 80 min, suggesting that adsorbent has reached equilibrium. Consequently, in the following adsorption experiments this time was used as the equilibration time.



**Fig. 3.** Adsorption kinetics of Cr(III) on adsorbent SPMF04. Conditions: [Cr(III)]<sub>0</sub> = 100, 200 and 400 mg L<sup>-1</sup>, 0.05 M Acetate buffer, pH = 3.60.

By analyzing the kinetic experiments allows us to elucidate the step that controls the rate for the chromium removal on SPMF04. The models studied involved chemical reaction and diffusion mechanisms such as film and intraparticle diffusion [41]. To achieve this goal, several adsorption mechanisms were tested with the experimental data. However, the film diffusion and intraparticle diffusion mechanisms did not explain satisfactorily the data; the mechanisms the adjusted better to the data are shown in this work, namely chemical reaction between chromium and the phosphonate functional groups (pseudo-first order and pseudo-second order kinetic mechanisms).

The pseudo-first order mechanism considers that there is a reversible reaction involved when a liquid is transferred to a solid phase with the equilibrium reached between the phases; this kinetics assumes that adsorbate accumulates on the surface of adsorbent as time goes on. Equation (2) represents the pseudo-first order rate [42]:

$$\ln (q_{\max} - q_t) = \ln q_{\max} - k_1 t \quad (2)$$

where,  $q_t$  is the adsorption uptake of chromium at time  $t$  ( $\text{mg g}^{-1}$ ) and  $k_1$  ( $\text{min}^{-1}$ ) is the rate constant of the pseudo-first order uptake. When plotting  $\log(q_{\text{max}} - q_t)$  vs time,  $k_1$  was calculated from the slope;  $k_1$  and  $R^2$  (Fig. 4a) are presented in table 3. This mechanism cannot predict  $q_{\text{max}}$  satisfactorily since the correlation coefficient is not close to unity, indicating a poor fit to data.

**Table 3.** Kinetic parameters for Cr (III) adsorption on adsorbent SPMF04.

| Initial concentration ( $C_0$ mg/L) | Pseudo-first order kinetics             |                             |        | Pseudo-second order kinetics            |  |        |
|-------------------------------------|---|-----------------------------|--------|---|--|--------|
|                                     | $q_{\text{max}}$ ( $\text{mg g}^{-1}$ ) | $k_1$ ( $\text{min}^{-1}$ ) | $R^2$  | $q_{\text{max}}$ ( $\text{mg g}^{-1}$ ) | $k_2$ ( $\text{g mg}^{-1} \text{min}^{-1}$ ) | $R^2$  |
| 93.15                               | 3.34                                    | 0.0105                      | 0.6042 | 20.06                                   | $8.89 \times 10^{-3}$                        | 0.9992 |
| 200.54                              | 9.15                                    | 0.0146                      | 0.7056 | 22.36                                   | $1.76 \times 10^{-3}$                        | 0.9914 |
| 421.65                              | 16.25                                   | 0.0126                      | 0.5317 | 39.14                                   | $5.31 \times 10^{-4}$                        | 0.9437 |

The pseudo-second order mechanism considers the removal capacity at equilibrium of a of system indicating that their removal capacity is comparable to the amount of active sites present [30]. Equation (3) represents the pseudo-second order rate. It can be expressed as:

$$\frac{t}{q} = \frac{1}{k_2 q_{\text{max}}^2} + \frac{t}{q_{\text{max}}} \quad (3)$$

where,  $q_{\text{max}}$  is the amount of adsorption at equilibrium ( $\text{mg g}^{-1}$ ) and  $k_2$  ( $\text{g mg}^{-1} \text{min}^{-1}$ ) is the rate constant of pseudo-second order adsorption. Fig. 4b depicts a graph of  $t/q$  versus  $t$  for Cr(III) on the adsorbent SPMF04. It can be seen from table 3 that correlation coefficient is higher than the corresponding one for the pseudo-first order case. These results indicate that the adsorption data are better fitted by the pseudo-second order mechanism.

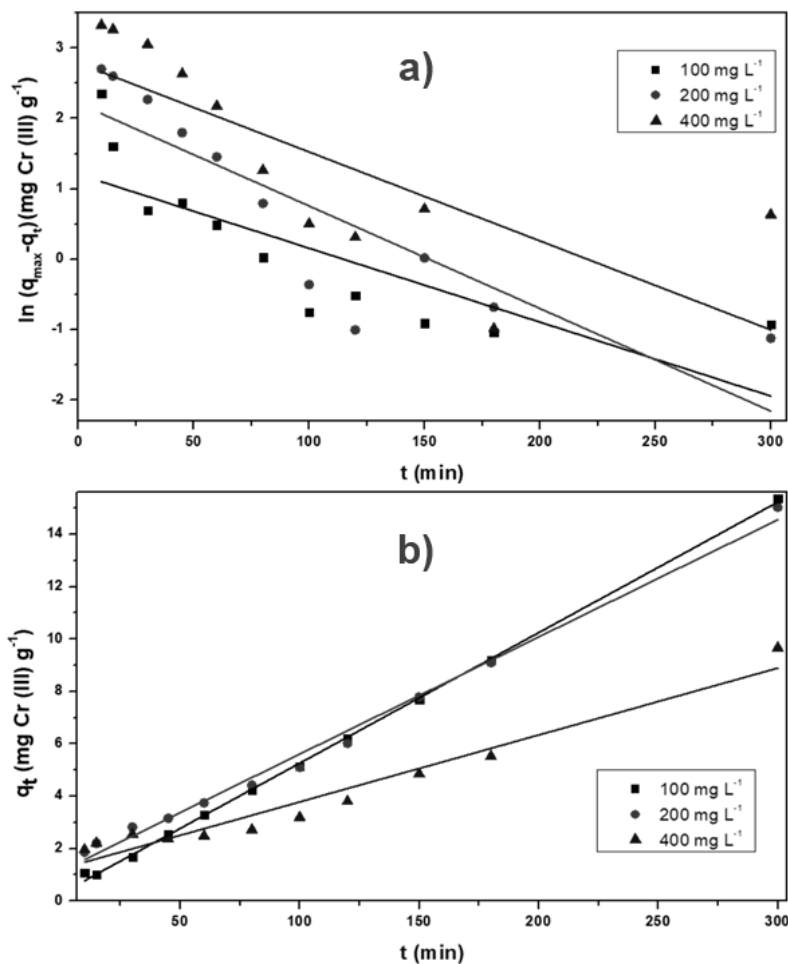


**Fig. 4.** Adsorption kinetic of Cr(III) on SPMF04: **a)** Pseudo-first-order model fit and, **b)** Pseudo-second-order model fit.

### Adsorption isotherms of Cr (III)

In order to obtain the Cr(III) removal capacity of adsorbent SPMF04 equilibrium isotherms were constructed. pH of solution effect on Cr(III) removal was studied at different pH's (3.13, 4.27 and 5.55) typical of industrial water discharges [43]. Fig. 5 shows the adsorption isotherms at 293 K for SPMF04. It can be observed that, as the acidity increases, the higher the Cr(III) removal; this is because the most likely species to be adsorbed,  $\text{Cr}(\text{CH}_3\text{COO})_2^+$ , is found in different percentages depending on the pH, for example at pH = 3, 25%, at pH = 4, 15% and at pH = 5, 5% (see speciation diagram in Supporting Information), this shows that at pH = 3.13 there are more  $\text{Cr}(\text{CH}_3\text{COO})_2^+$  species and therefore a higher probability of being adsorbed on the surface of the material. In order to help explain the adsorption mechanism, the zero point charge (ZPC) experiment was carried out, the value obtained was  $\text{pH}_{\text{zpc}} = 7.6$  (plot included in the Supporting Information), it implies that below this pH value the phosphonic species are present and then, the possible uptake mechanism is by means of proton transfer between phosphonic acid and the  $\text{Cr}(\text{CH}_3\text{COO})_2^+$  with proton releasing to the medium. This is corroborated with the decrease of the pH after the adsorption process. A regeneration step of adsorbent SPMF04 was carried out by using 50 cm<sup>3</sup> of 1.0 M HCl solution with ~92% of the chromium recovered; sample did not dissolve with this acid.

Langmuir and Freundlich equations have been applied to a great variety of sorption processes. Langmuir isotherm works perfectly in the processes of monolayer adsorption where it is considered that at

any point on the surface of material there is the same activity of adsorption of each molecule on the surface, while Freundlich isotherm considers a heterogeneous surface where the magnitude of adsorption heat varies exponentially with the covering of the surface and expresses a multimolecular adsorption. Langmuir and Freundlich equations can be expressed, respectively, as [44]:

$$q_e = \frac{K_L C_e q_{\max}}{1 + K_L C_e} \quad (4)$$

$$q_e = K_F C_e^{1/n} \quad (5)$$

where,  $q_e$  ( $\text{mg g}^{-1}$ ) is the equilibrium removal capacity of adsorbent;  $C_e$  represents the equilibrium concentration of the chromium ions ( $\text{mg L}^{-1}$ ),  $q_{\max}$  is the maximum amount of Cr(III) removal ( $\text{mg g}^{-1}$ ),  $K_L$  the adsorption equilibrium constant ( $\text{L mg}^{-1}$ ),  $K_F$  is a constant that indicates the sorption capacity ( $\text{mg g}^{-1}$ ) ( $\text{L mg}^{-1}$ )<sup>1/n</sup>,  $n$  is a constant indicating the sorption intensity. Fig. 5 shows the adsorption curves isotherms of chromium ions. Values of parameters from the Langmuir and Freundlich equations obtained from the regressions are shown in table 4. The Cr(III) removal capacities of adsorbent SPMF04 augment as the chromium concentration increases. In general, it can be observed that in the case of Langmuir equation, coefficient  $R^2$  tends to 1 compared to those of Freundlich equation obtaining a better fit of data in the case of Langmuir equation. Elucidation of chromium-phosphonate surface complex is obtained from the aqueous phase chemical equilibrium (see Supplementary material), FTIR, and XPS results.

**Table 4.** Freundlich and Langmuir isotherm constants and correlation coefficients on adsorbent SPMF04 .

| pH   | Freundlich  |      |                | Langmuir                          |                              |                |
|------|---|------|----------------|-----------------------------------|------------------------------|----------------|
|      | $K_F$ ( $\text{mg g}^{-1}$ )<br>( $\text{L mg}^{-1}$ ) <sup>1/n</sup> | n    | R <sup>2</sup> | $q_{\max}$ ( $\text{mg g}^{-1}$ ) | $K_L$ ( $\text{L mg}^{-1}$ ) | R <sup>2</sup> |
| 3.13 | 2.37  | 2.49 | 0.8195         | 34.37                             | 0.01306                      | 0.9863         |
| 4.27 | 2.10  | 3.10 | 0.7873         | 18.87                             | 0.01091                      | 0.9832         |
| 5.55 | 3.24  | 7.42 | 0.9418         | 8.44                              | 0.02242                      | 0.9987         |

With the aim of comparing the properties of synthesized adsorbents from this work with the ones from reports from the literature, in table 5 are shown the adsorption capacities of adsorbents produced to extract Cr(III) from aqueous streams. In this study, incorporation of SPMF with crosslinking agent TEOS was carried out without the need of SPMF hydrolysis, thus representing an advantage compared to SOL-PHONIC material in which the functional group trimethoxysilyl propyl diethyl phosphonate requires to be synthesized from other precursors. On the other hand, the material CTPP shows a high Cr(III) uptake capacity, however, the equilibrium time is around 3 days whereas in the case of SPMF04 is of the order of 80 min. This implies that SPMF04 shows a relatively lower resistance to mass transfer and that its operating conditions are more suitable to be employed in adsorption systems of packed beds. On the other hand, table 5 also shows the maximum chromium capacity of two cheap, easily tuned (regarding physicochemical properties and available as raw materials) adsorbents Zeolite NaX and GMZ bentonite, however, these adsorbents show a lower chromium removal compared to SPMF.

**Table 5.** Comparison of Cr(III) uptake using adsorbent SPMF04 with different materials.

| Material         | $q_{\max}$<br>mg Cr(III) g <sup>-1</sup> | Supporting Material<br>/Functional group | Reference |
|------------------|--|--|-----------|
| SOL-PHONIC       | 82                                       | Silica/Phosphonic acid                   | [70]      |
| SPMF04           | 78.6                                     | Silica/Methylphosphonate                 | This work |
| CTPP             | 124                                      | Chitosan/ tripolyphosphate               | [71]      |
| Algae biomass    | 34                                       | Biomass/ Algae biomass                   | [72]      |
| Activated carbon | 31.5                                     | Carbon/Oxidated carbon                   | [73]      |
| Zeolite NaX      | 62.56                                    | Cation exchange                          | [74]      |
| GMZ bentonite    | 4.68                                     | Cation exchange                          | [75]      |

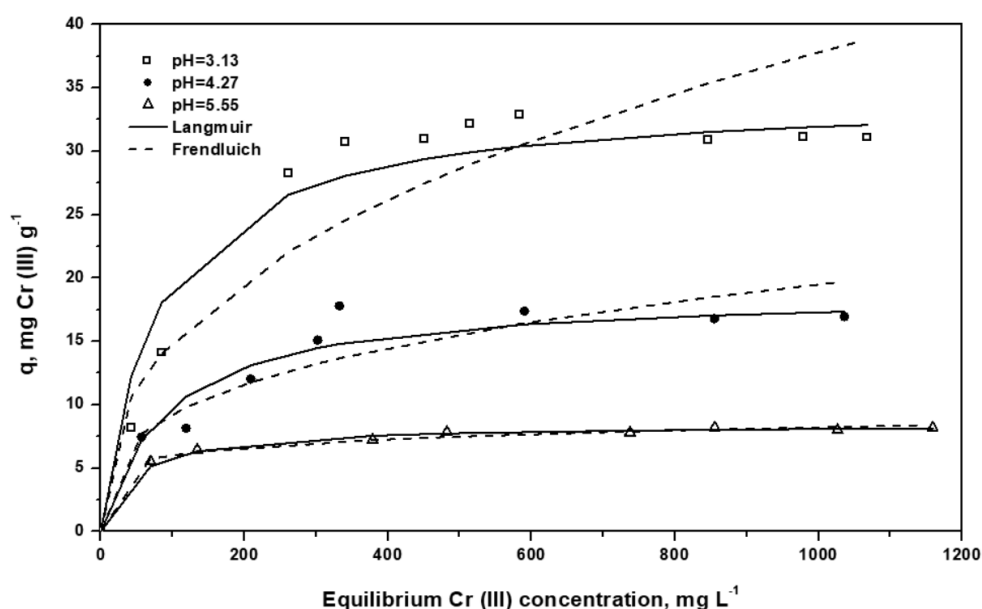
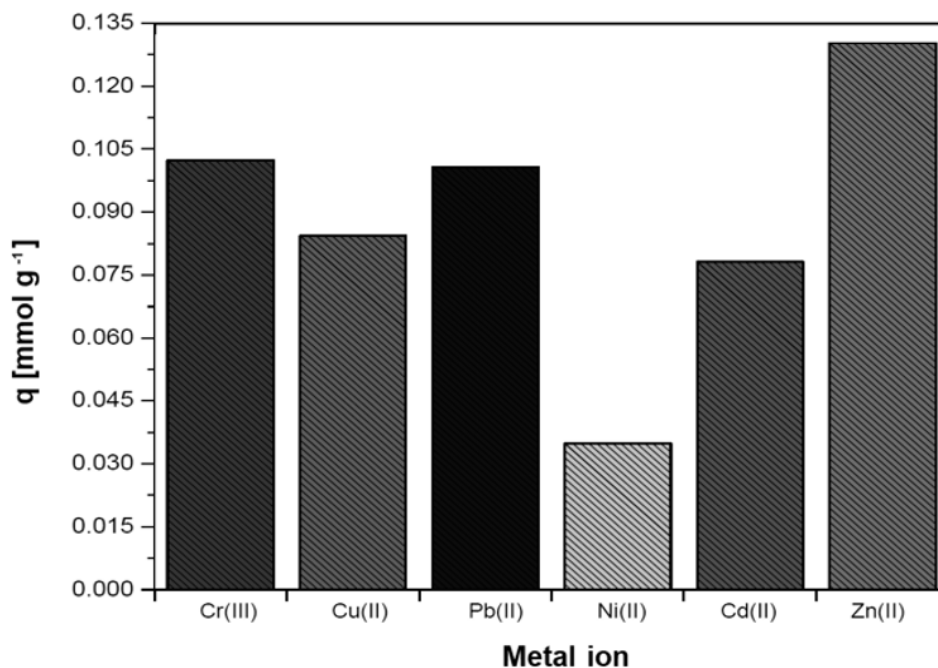


**Fig. 5.** Adsorption isotherms at three equilibrium pH values on adsorbent SPMF04. Experimental conditions: volume 50 mL, adsorbent weight = 0.20 g, T = 303 K.

### Selectivity measurements

The purpose of these measurements was to determine the selectivity of phosphonate group on adsorbent SPMF04 towards Cr(III) while other metals are present. Selectivity of this adsorbent for six potentially toxic metals studied (Cr(III), Cd(II), Cu(II), Pb(II), Ni(II), Zn(II)) is shown in Fig. 6. It can be observed from this figure that the material presented a higher preference for Zn(II) followed by Cr(III), which has a little higher or equal affinity to that of Pb(II). The general trend observed is in the order of Zn > Cr > Pb > Cu > Cd > Ni. These results show that the adsorbent has potential application in the uptake of Cr(III), Zn(III) and Pb(II) from the aqueous phase. On the other hand, Sheng et al indicate that affinity of metal ions for the functional groups present on the adsorbent, can be associated to the electronegativities of the metal ions present [45], since a lower electronegativity means that metal ion shows a greater attraction for the free electrons on the ligands of the functional groups. However, the presence of acetate buffer in the solution alters

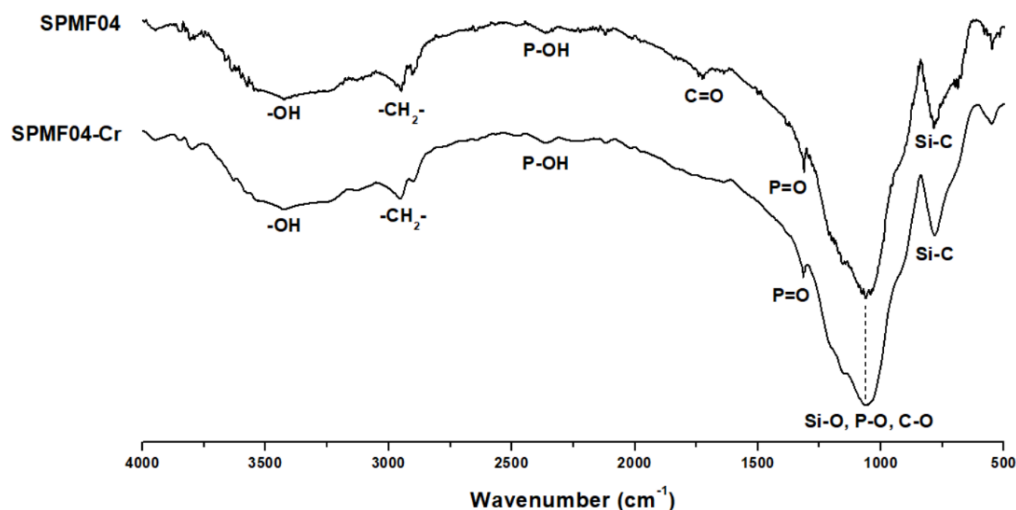
the chemical affinity of metal ions, since in addition to the electronegativity effect; cationic competition will also depend on the acetate-metal complex formed.



**Fig. 6.** Selectivity of metal ions on the surface of adsorbent SPMF04. pH = 3.64. T = 25°C.

### FTIR results

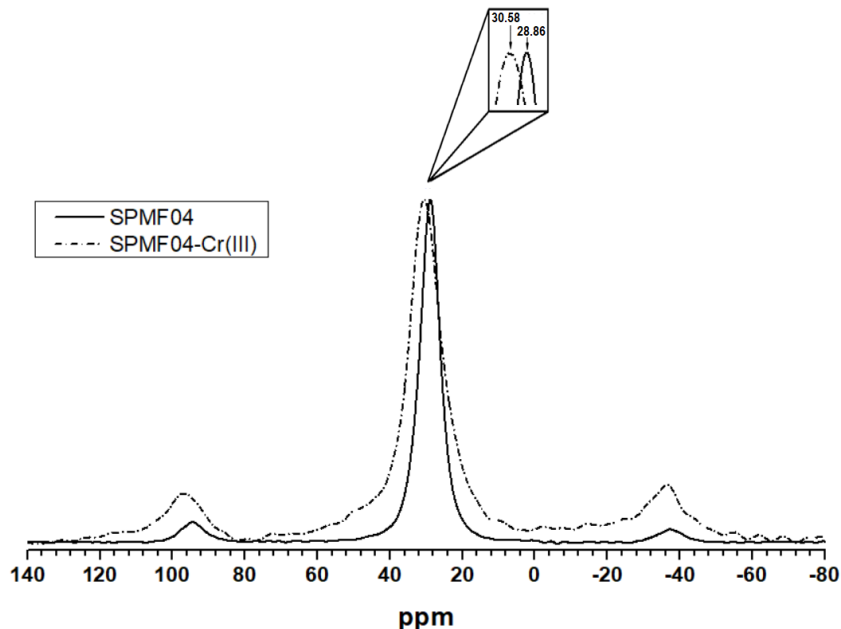
The FTIR spectra are shown in Fig. 7. Characteristic signals related to the chemical composition of each sample are observed in the spectra. For example, the two spectra (SPMF04 and SPMF04-Cr) exhibit a wide and intense signal at 3400 cm<sup>-1</sup> corresponding to stretching vibrations of OH groups from silanols attached to the surface of adsorbent [46]. The wide and intense band at 1030-1180 cm<sup>-1</sup> is due to stretching vibrations of siloxane groups ( $\equiv\text{Si}-\text{O}-\text{Si}\equiv$ ) of the silica matrix structure [46]–[48] as well as C-O and P-O bonds of the phosphonate moieties [47]. The band at 2950 cm<sup>-1</sup> is caused by the asymmetric stretching of the C-H from the  $-\text{CH}_2-$  group [27], [47]. A peak at 785 cm<sup>-1</sup> is due to the Si-C bond [47]. The bands at around 2325 and 1320 cm<sup>-1</sup> are due to stretching vibrations of P-OH and P=O bonds, respectively, indicating the presence of phosphonate group on the surface of adsorbent. Moreover, the presence of a band at 2325 cm<sup>-1</sup> corresponding to the P-OH group evidences that not all phosphonic acid groups were converted to sodium salt of phosphonates during synthesis of the material. In the case of spectrum of adsorbent with chromium (SPMF04-Cr), a small band appeared at 1726 cm<sup>-1</sup> corresponding to the stretching vibration of carbonyl group (C=O) of the acetate groups [47], in agreement with the aqueous phase chemical speciation (see Supporting material), which suggests that the ions of chromium diacetate  $\text{Cr}(\text{CH}_3\text{COO})_2^+$  and/or divalent chromium acetate  $\text{Cr}(\text{CH}_3\text{COO})^{+2}$  are the potential aqueous species to be adsorbed at the experimental conditions studied.



**Fig. 7.** FTIR spectra of the adsorbent before (SPMF04) and after the adsorption process (SPMF04-Cr).

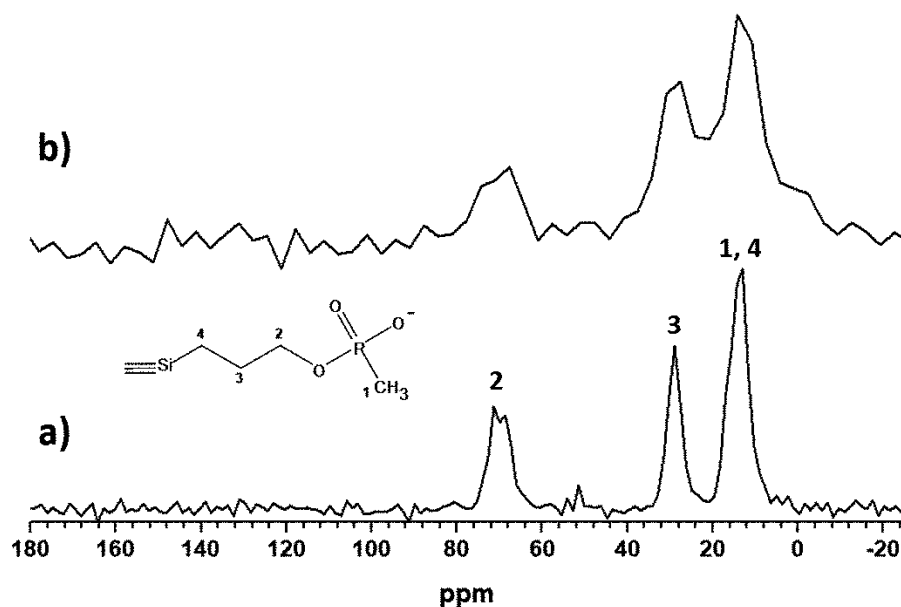
### Solid state NMR analysis results

Fig. 8 shows the MAS  $^{31}\text{P}$ -NMR spectra of the adsorbent SPMF04 and the adsorbent after the chromium adsorption process (SPMF04-Cr). Both spectra depict a principal signal located at 28.8 ppm for sample SPMF04 and at 30.58 ppm in the case of the sample with chromium (SPMF04-Cr). Small symmetrical signals around 95 and -39 ppm correspond to classical spinning side bands (SSB) in a MAS experiment (8KHz). In general, three differences due to the presence of Cr(III) in the sample are observed: 1) signal broadening (dash dot line), 2) isotropic signal shifting from 28.8 to 30.58 ppm (see expanded zone, Fig. 8) and 3) side bands intensity. It can be explained as chromium ions adsorbed on the sample cause changes in the local environment of the phosphorus nuclei which promotes an increase in the chemical shift anisotropy (CSA) [49] as well as in the dipolar coupling interactions [76, 77]. In other words, all these changes observed in the SPMF04-Cr spectrum resulted from an effective interaction between phosphate moieties and chromium ions. Furthermore, higher SSB intensity is also attributed to the heteronuclear dipolar coupling (I,S) between a spin-1/2 nucleus ( $^{31}\text{P}$ ) and a quadrupolar spin-3/2 nucleus ( $^{53}\text{Cr}$ ) [78-80]. This clearly contributes with the anisotropy of the two spin system, since all quadrupolar nuclei exhibited an electric field gradient (EFG) tensor. This could be influencing directly the local electronic environment of spin-1/2 nuclei ( $^{31}\text{P}$ ) due to the chromium proximity matches with the I-S internuclear distances range ( $r^2$ ). In summary,  $^{31}\text{P}$ -NMR spectra analyses of the SPMF04 and SPMF04-Cr samples confirmed in which level the metal uptake is taking place.



**Fig. 8.** Solid-state MAS <sup>31</sup>P NMR for SPMF04 and SPMF04-Cr(III) samples.

CPMAS <sup>13</sup>C-NMR spectra of the carbonated organic ligand in the samples SPMF04 and SPMF04-Cr are depicted in Fig. 9 a and b, respectively. In the spectrum of SPMF04 it can be observed three principal signals located at around of 67, 24 and 10 ppm due to the different carbon environments in the sample. According to the ligand structure in the Fig 9a, the signal at 67 ppm corresponds to carbon 2 which is attached to oxygen. In the case of signal at around 24 ppm is attributed to carbon labeled as 3 from the propyl chain and finally, signal located at the highest field (10 ppm) is obtained from two carbons 1 (C-Si) and 4 (C-P) with closer chemical shifts (overlapped signals). Spectrum b of Fig. 9 corresponds to sample of adsorbent after chromium treatment (SPMF04-Cr). In general, the same signal pattern is observed and only the intensity of the signals changes in comparison with the original adsorbent (spectrum a). This effect can be due to the presence of the metal onto the organic ligand affecting the relaxation time of the carbons (T1) and in consequence, the signal intensities. On other hand, signals from acetate groups related to chromium are not distinguishable as in FTIR analysis because of practical difficulties. This means that carbon signal of methyl group from acetate overlap with the signal at 24 ppm of carbon 3 (similar chemical shift) and the carbonyl signal is not observable due to the low acetate concentration in the sample and also to the longer T1 typical of the carbonyl groups in solid state. Furthermore, no signals at 19 and 60 ppm due to remaining ethoxy groups (CH<sub>3</sub>-CH<sub>2</sub>-O-) are observed as a confirmation of the complete hydrolysis of the TEOS during the synthesis of the silicate matrix.



**Fig. 9.** CPMAS  $^{13}\text{C}$  NMR spectra of samples: **a)** SPMF04 and, **b)** SPMF04-Cr.

Fig. 10 depicts the MAS  $^{29}\text{Si}$  NMR spectra of the samples of adsorbents SPMF04 (a) and SPMF04-Cr (b) before and after chromium uptake process, respectively. In the spectra two groups of signals corresponding to the silicon species T and Q are appreciated. Signals located at -59 and -68 ppm are originated from  $\text{T}^2$  and  $\text{T}^3$  species which confirms the presence of the phosphonate ligand in the adsorbents (see structures in the upper part of Fig. 10). Signals attributed to Q species of the silicate matrix are  $\text{Q}^3$  with a remaining silanol group ( $\equiv\text{Si-OH}$ ) at -102 ppm and  $\text{Q}^4$  at -111 ppm from the silicon oxide matrix (upper part of Fig. 10). The area corresponding to each signal of the silicon species as well as the percentage of each species in the pristine adsorbent (SPMF04) is as follows: the highest percentage is obtained with  $\text{T}^3$  species with 63.9% followed by  $\text{T}^2$  with 22.0%. In contrast, each Q species represent less than 10% in the sample ( $\text{Q}^3 = 4.5\%$  and  $\text{Q}^4 = 9.6\%$ ). These results indicate that the inorganic silicate matrix is a narrow layer in comparison with the high presence of the phosphonate organic ligand. In other words, the 1:1 molar ratio of TEOS/SPMF used in the synthesis of the SFMF04 adsorbent does not correspond to the relation between species T and Q of the final material. It can be explained as the synthesis conditions promoted principally the linkage between silicated functional ligands (between T species) in instance to form the silicon oxide matrix from TEOS (Q species). Signal intensity of T and Q species decreased when the adsorbent sample contains Cr(III) as can it be appreciated from the spectrum b of Fig. 10. This effect is noticeable in the signals at -59 and -68 ppm ( $\text{T}^2$  and  $\text{T}^3$ , respectively) where is clearly expected to find chromium associated to phosphonate moieties. However, the signal intensity of  $\text{Q}^3$  is also modified due to the presence of the silanol groups which can also be affected by Cr(III). In contrast,  $\text{Q}^4$  does not seem to be affected because of the lack of silanol groups in the silicate matrix.

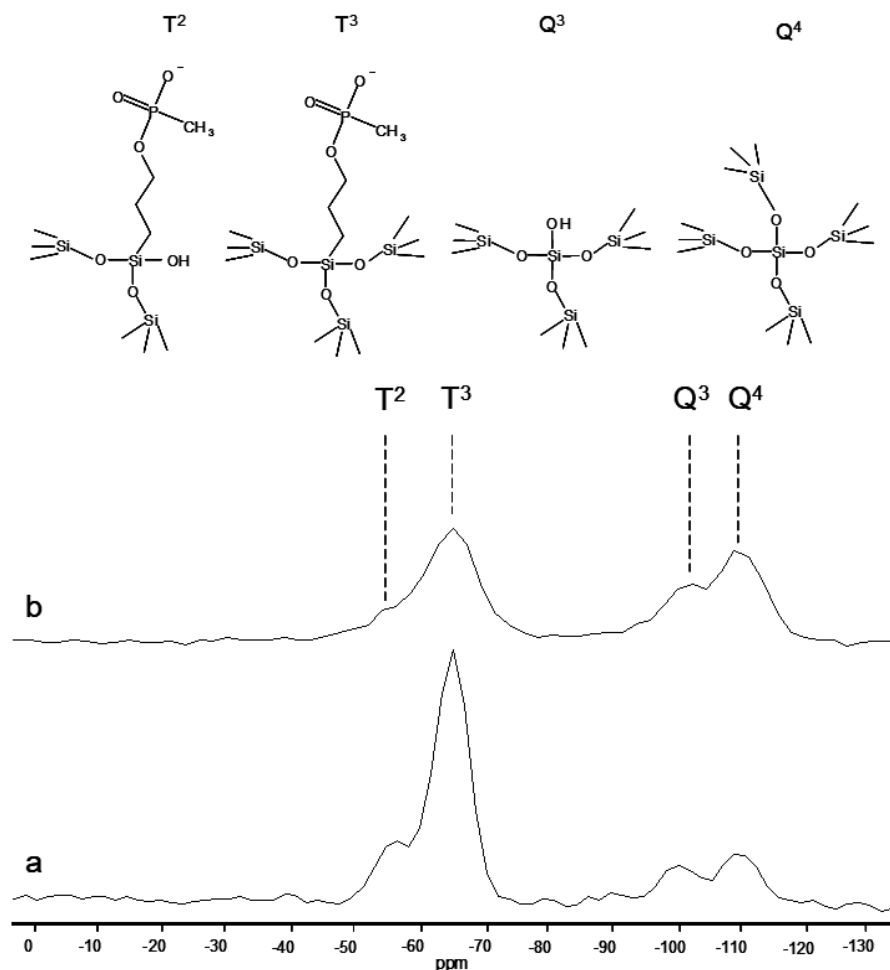


**Fig. 10.** MAS  $^{29}\text{Si}$  NMR spectra of samples: **a)** SPMF04, and **b)** SPMF04-Cr. Upper part: structures of T and Q silicon species.

### XPS analysis results

The prepared adsorbent SPMF04 was investigated by XPS with chromium and pristine with the aim of determining the chemical environment and the types of elements participating in the adsorption process. Fig. 11 shows the wide-scan XPS spectra of pristine material (SPMF04) and of the adsorbent with chromium removed (SPMF04-Cr). The signals noticed correspond to O1s, C1s, P 2p, Na 1s, and Cr 2p. It is evident a new peak at binding energy (BE) of 535 eV after Cr removal. The C 1s spectrum of SPMF04 (Fig. 12a) was fitted with four components centered at 283.0, 284.3, 285.5 and 287.3 eV, associated to carbon atoms in C-Si [52], [53], C-C [54], [55], C-O [52], [56], and C-P [55], [57]. These signals then correspond to carbon in the propyl chain (C-Si, C-C and C-O) and the methyl linked to the phosphonate group (C-P). The carbon spectrum in SPMF04-Cr(III) (Fig. 12b) required five components: three of them at 282.8, 284.5 and 285.57 eV attributed to carbon in C-Si, C-C, and C-O bonds; another signal at 287.4 eV due to the C-P bond observed in the pristine adsorbent; and finally the signal at 284.3 eV can be associated to alpha carbons in acetate groups [27], [53]. These components confirm the presence of acetate groups after the adsorption process suggesting that chromium is retained in the acetate form. The analysis of the O 1s spectrum in SPMF04 (Fig. 12c) revealed components at 533.86 and 531.5 eV of oxygen bonded to C-O-P [58] and P=O. At 532.6 eV rises the spectrum when oxygen is bonded to silicon in the silica structure [53], [59] and to phosphorus in the protonated phosphonic groups [55], [57], thus this signal might result as an overlap of both

signals. Additionally, the signal at 530.1 eV is associated to oxygen in P-O-Na [60], and this confirms the presence of phosphonate groups, which were not protonated. The spectrum in the SPMF04-Cr(III) sample (Fig. 12d) presented signals of oxygen in C-O-P (533.4 eV) and P=O (531.1 eV) as well as the band produced simultaneously by Si-O and P-OH at 532.1 eV also found in SPMF-04. A new component at 530.0 eV, which is typical of oxygen in P-O-Cr [57], along with that at 531.1 eV assigned to C=O [53] reinforce the speciation analysis indicating the stability of chromium acetate species and evidence that acetate is the most probable form in which chromium is retained by the adsorbent. The spectrum of phosphorus corresponding to the 2p core-level (Fig. 13a) in SPMF-04 was fitted with three components. One at 133.4 eV attributed to phosphorus linked to oxygen in P=O and P-OH at 133.4 eV [62] and P-O-C [63], [64]. The other components at 132.0 and 135.0 eV are related to phosphorus in P-C [65] and P-O-Na [66], therefore the presence of phosphonic and sodium phosphonate groups in the adsorbent is confirmed. The adsorption of chromium induced significant changes in the P 2p spectra (Fig. 13b), once the P-O-Na signal at 135.0 eV was not detected, thus the  $-\text{PO}_3\text{Na}$  groups are forming complexes with chromium acetate or they were protonated once the final pH after the adsorption experiments (pH = 2.98) was enough to produce the protonated form. At higher pH, the presence of sodium phosphonate groups is favored but we observe experimentally that the adsorption capacity diminishes. The components in this SPMF04-Cr sample at 132.5 eV correspond to P-C; the one at 133.9 eV is attributed to P=O and P-OH, and that at 133.9 eV belongs to P-OC and P-OCr [67]. Therefore, the anchoring of chromium acetate to the adsorbent occurs through phosphonic/phosphonate groups. Before the adsorption experiment, the adsorbent presented a spectrum band at 1071.7 eV which is typical of the 1s core level in sodium atoms (see sample SPMF04 in Fig. 13c). The spectrum from the Cr 2p core-level was collected from the SPMF04-Cr(III) sample (Fig. 13d). The doublet composed by signals at 577.4 and 586.7 eV corresponds to Cr 2p<sub>3/2</sub> and Cr 2p<sub>1/2</sub> and these values have been earlier observed in chromium acetate [18], [68], [69] confirming the presence of divalent or trivalent chromium, in agreement with FTIR results and aqueous phase chemical equilibrium (see Supporting material).

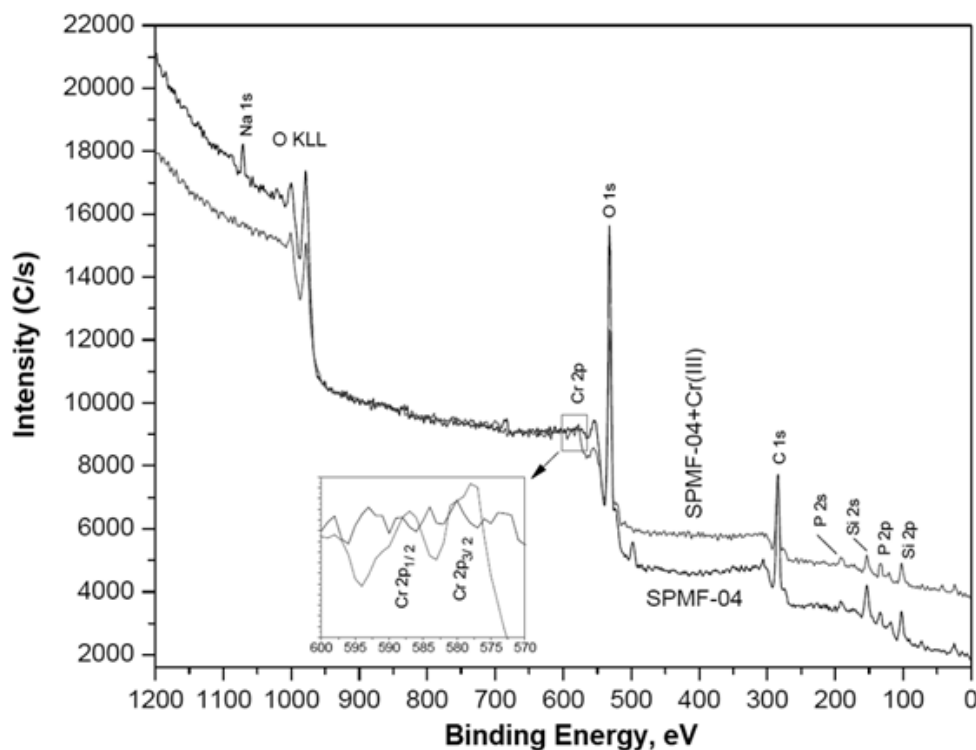
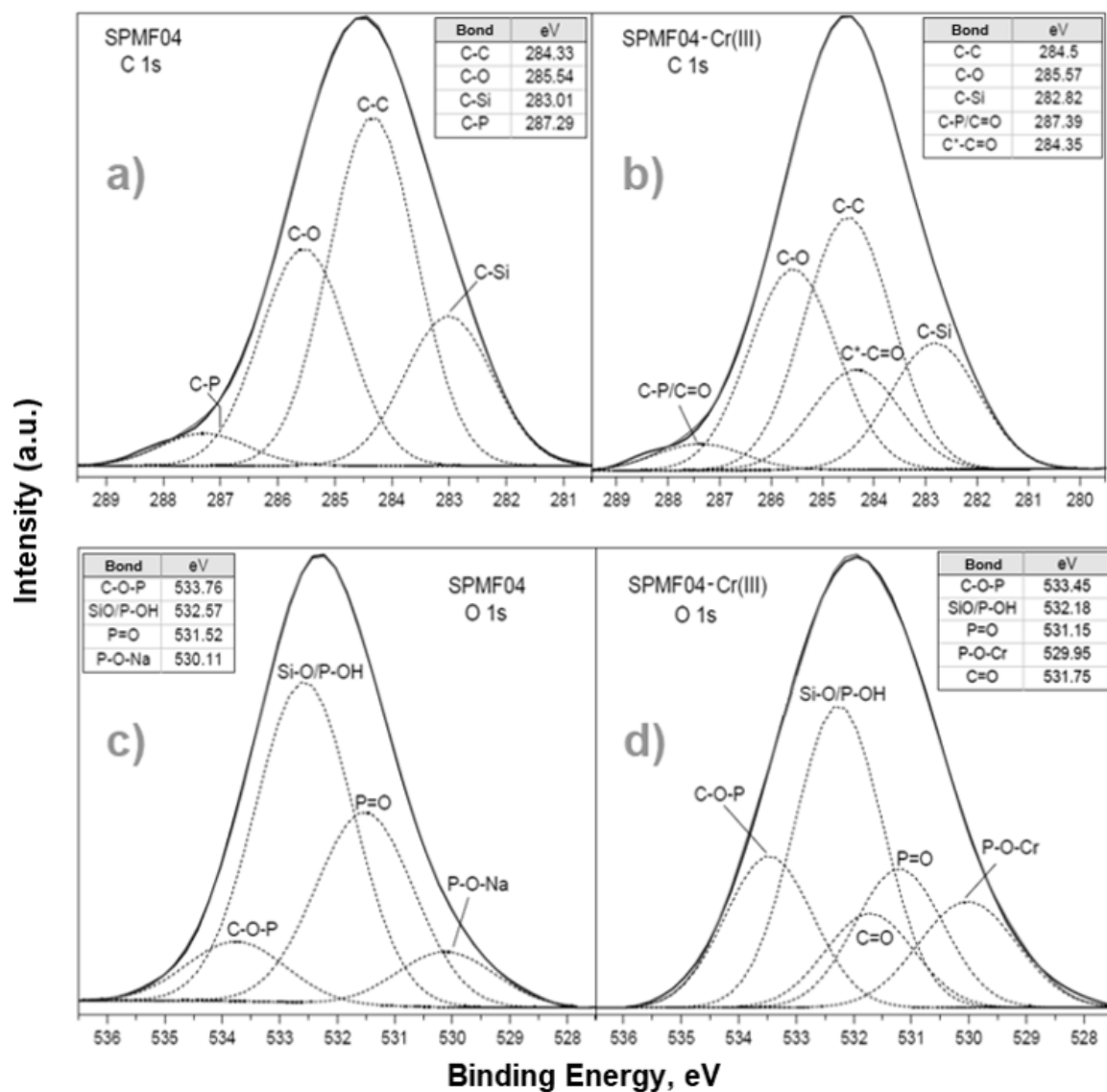
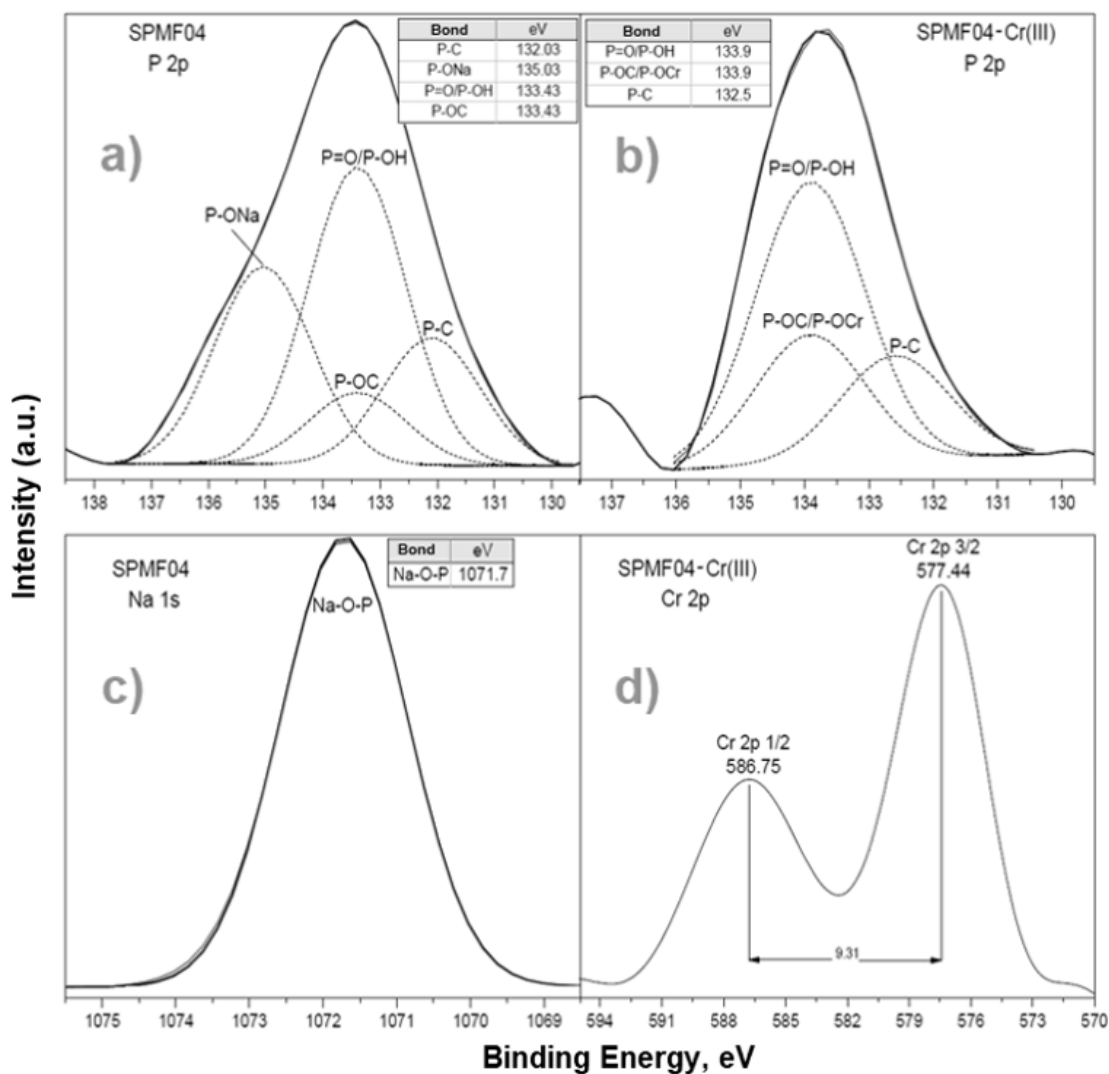


Fig. 11. XPS wide scan spectra of SPMF04 and SPMF04-Cr(III).



**Fig. 12.** XPS spectra of: a) C 1s SPMF04, b) C 1s SPMF04-Cr(III), c) O 1s SPMF04, and d) O 1s SPMF04-Cr(III).



**Fig. 13.** XPS spectra of: **a)** P 2p on SPMF04, **b)** P 2p on SPMF04-Cr(III), **c)** Na 1s on SPMF04 and **d)** Cr 2p on SPMF04-Cr(III).

## Conclusions

In this work, insight into chromium removal chemistry on phosphonate-functionalized silica was studied. The synthesis of adsorbents with high ligand densities of phosphonate groups ( $2.923 \text{ mmol P g}^{-1}$ ) in the range of mesopores was shown from the elemental analysis and nitrogen uptake experiments. The adsorbents were synthesized by co-condensing reactions between SPMF and TEOS. Monovalent dichromate acetate ( $\text{CrAc}^+_2$ ) was the species removed from the aqueous solution, according to the speciation aqueous phase chemical equilibrium, FTIR and XPS results. The highest Cr(III) removal by SPMF04 adsorbent was  $78.639 \text{ mg g}^{-1}$  at pH 3.6. SPMF04 adsorbent presented enhanced chromium removal capacity in comparison to solid adsorbents possessing different complexing moieties found in the literature. Removal of Cr(III) ions was fast, as observed from kinetic measurements. The attraction toward Cr(III) (as  $\text{CrAc}^+_2$ ) when other metal ions were present in the solution followed the order of  $\text{Zn(II)} > \text{Cr(III)} \geq \text{Pb(II)} > \text{Cu(II)} > \text{Cd(II)} > \text{Ni(II)}$ .

The presence of phosphonate ligands on the surface of SPMF04 adsorbent interacting with Cr(III) ions (as  $\text{CrAc}^+_2$ ) was demonstrated from FTIR, NMR and XPS analyses. Finally, the signal intensity of Q3 species from the NMR measurements, was also modified due to the presence of the silanol groups which can also be affected by the presence of Cr(III).

## Acknowledgments

Financial support is acknowledged to Mexico's National Council for Science and Technology (CONACyT) through grants CB-84252 and INFR3 174186 and a scholarship given to P.I. Hernandez-Velazquez. We thank Mr. F. Lopez-Herrera y Cairo for his help in conducting the  $\text{N}_2$  adsorption measurements.

## References

1. L. Khezami and R. Capart. *J. Hazard. Mater.*, **2005**, 123, 1, 223–231.
2. P. A. Kobielska, A. J. Howarth, O. K. Farha, and S. Nayak. *Coord. Chem. Rev.*, **2018**, 358, 92–107.
3. P. Taylor, I. Narin, M. Soylak, K. Kayakirilmaz, L. Elci, and M. Dogan. *Anal. Lett.*, **2014**, 35, 37–41.
4. G. Bayramoglu and M. Y. Arica. *J. Hazard. Mater.*, **2011**, 187, 1–3, 213–221.
5. B. Gordon, P. Callan, and C. Vickers, **2008**, *WHO Chron.*, 38, 3, 564.
6. T. N. De Castro Dantas, A. A. D. Neto, and M. C. P. De A. Moura. *Water Res.*, **2001**, 35, 9, 2219–2224.
7. M. Costa. *Toxicology and Applied Pharmacology*, **2003**, 188,1, 1–5.
8. M. Ezoddin, F. Shemirani, and R. Khani. *Desalination*, **2010**, 262, 1–3, 183–187.
9. A. M. Farag, May, T., Marty, G. D., Easton, M., Harper, D. D., Little, E. E., Cleveland, L. *Aquat. Toxicol.*, **2006**, 76, 3–4, 246–257.
10. D. E. Kimbrough, Y. Cohen, A. M. Winer, L. Creelman, and C. Mabuni. *Critical Reviews in Environmental Science and Technology*, **1999**, 29, 1, 1–46.
11. S. Kocaoba and G. Akcin. *Adsorption*, **2003**, 9, 2, 143–151.
12. A. Puri and M. Kumar. *Indian J. Occup. Environ. Med.*, **2012**, 16, 1, 40.
13. [A. Duran, M. Tuzen, and M. Soylak. *Food Chem. Toxicol.*, **2011**, 49, 7, 1633–1637.
14. Report EPA 815-R-03-002, Washington, DC., **2003**.
15. C. Földi, R. Dohrmann, K. Matern, and T. Mansfeldt. *J. Soils Sediments*, **2013**, 13, 7, 1170–1179.
16. D. Dias, N. Lapa, M. Bernardo, W. Ribeiro, I. Matos, I. Fonseca, F. Pinto. *Bioresource Technol.* **2018**, 139–150.
17. S. Sainia, Simarpreet Arora, Kirandeep, Bhupinder Pal Singh, Jatinder Kaur Katnoria, Inderpreet Kaur. *J Environ Chem Eng.* 6, 2, **2018**, 2965–2974.
18. E. Aranda-García, Eliseo Cristiani-Urbina. *Environ Sci Pollut Res*, **2019**, 26:3157–3173
19. L. Ayele, Eduardo Pérez, Álvaro Mayoral, Yonas Chebude, Isabel Díaz. *J Chem Technol Biotechnol.* 93, 1, **2018**, 146–154.
20. V. Shojaei, Hamid Khoshdast. *Physicochem. Probl. Miner. Process.*, **2018**, 54(3), 1014–1025.
21. S. Vasudevan, Lakshmi, J., Sozhan, G. *Clean-Soil Air Water.* **2009**, 37, 45–51.
22. E. Bazrafshan, Moein, H., Mostafapour, F.K., Nakhaie, S. *J. Chem.* **2013**, 2013, 640139.
23. O. Sahu, Mazumdar, B., Chaudhari, P.K. *Environ. Sci. Pollut. Res.* **2014**, 21, 2397–2413.
24. J. Kyzioł-Komosińska, Joanna Augustynowicz, Wojciech Lasek, Justyna Czupioł, Daniel Ociński, *J. Environ. Manage.* 214, **2018**, 295–304.
25. R. O. Ogbodu, Martins O. Omorogie, Emmanuel I. Unuabonah, Jonathan O. Babalola. *Environ Prog Sustain Energy.* 34,6, **2015**, 1694–1704.
26. A. Shukla, S. Srivastava, S. F. D'Souza. *Int. J. Environ. Sci. Technol.* 2018, 15:2701–2712.
27. C. A. Quirarte-Escalante, V. Soto, W. De La Cruz, G. R. Porras, R. Manriquez, and S. Gomez-

- Salazar. *Chem. Mater.*, **2009**, 21, 8, 1439–1450.
28. S. E. Gomez-Gonzalez, G. G. Carbajal-Arizaga, R. Manriquez-Gonzalez, W. De la Cruz-Hernandez, S. Gomez-Salazar, *Mater. Res. Bull.*, **2014**, 59, 394–404.
29. P. Yin, Tian, Y., Wang, Z., Qu, R., Liu, X., Xu, Q., Tang, Q. *Mater. Chem. Phys.*, **2011**, 129, 1–2, 168–175.
30. Y. Liu, L. Guo, L. Zhu, X. Sun, and J. Chen. *Chem. Eng. J.*, **2010**, 158, 2, 108–114.
31. J. S. Lee and L. L. Tavlarides. *Solvent Extr. Ion Exch.* **2002**, 20, 3, 407–427.
32. J. S. Lee, S. Gomez-Salazar, and L. L. Tavlarides, *React. Funct. Polym.*, vol. 49, no. 2, pp. 159–172, **2001**.
33. U. Schubert, N. Hiising, and A. Lorenz. *Chem. Mater.*, **1995**, 7, 11, 2010–2027.
34. M. Streat. *React. Funct. Polym.*, **1998**, 38, 219–226.
35. B. Liu, Y. Fang, and M. Terano. *J. Mol. Catal. A Chem.*, **2004**, 219, 1, 165–173.
36. C. Brinker and G. Scherer. *Sol-Gel Science: The Physics and Chemistry of Sol-Gel Processing*, **1990**.
37. J. S. Lee and L. L. Tavlarides. New York: 14, Ch. 5. Marcel Dekker, **2001**.
38. M. Thommes, Kaneko, K., Neimark, A. V, Olivier, J. P., Rodriguez-reinoso, F., Rouquerol, J., Sing, K. S. W. IUPAC Technical Report, 87, 1051–1069, **2015**.
39. L. L. Hench and J. K. West. *Chem. Rev.*, **1990**, 90, 1, 33–72.
40. R. Deshpande, D.-W. Hua, D. M. Smith, and C. J. Brinker. *J. Non. Cryst. Solids*, **1992**, 144, 32–44.
41. H. Chen and A. Wang. *J. Hazard. Mater.*, **2009**, 165, 1–3, 223–231.
42. Y. Niu, Qu, R., Chen, H., Mu, L., Liu, X., Wang, T., Sun, C. *J. Hazard. Mater.*, **2014**, 278, 267–278.
43. S. Sreesai and S. Sthiannopkao. *Can. J. Civ. Eng.*, **2009**, 719, 709–719.
44. J. Zhang, Zhai, S., Li, S., Xiao, Z., Song, Y., An, Q., Tian, G. *Chem. Eng. J.*, **2013**, 215–216, 461–471.
45. P. X. Sheng, Y.-P. Ting, and J. P. Chen. *Ind. Eng. Chem. Res.*, **2007**, 46, 8, 2438–2444.
46. G. Socrates. Infrared and Raman characteristic group frequencies. <https://doi.org/10.1002/jrs.1238>
47. D. L. Pavia, G. M. Lampman, and G. S. Kriz, Harcourt College Publishers, **2001**.
48. D. J. K. Robert M. Silverstein, Francis X. Webster, *Spectrometric identification of organic compounds*. **2005**.
49. D. A. Skoog, F. J. Holler, T. A. Nieman, and M. C. M. Gómez, McGraw-Hill, **2000**.
50. J.-P. Mercier, P. Morin, M. Dreux, and A. Tambute. *Chromatographia*, **1998**, 48, 7, 529–534.
51. H.-F. Klein. *Angew. Chemie Int. Ed.*, **2005**, 44, 45, 7331.
52. S. Deshpande, S. Dakshinamurthy, S. C. Kuiry, R. Vaidyanathan, Y. S. Obeng, and S. Seal. *Thin Solid Films*, **2005**, 483, 1–2, 261–269.
53. M. A. Sharif and H. Sueyoshi. *Ceram. Int.*, **2009**, 35, 1, 349–358.
54. K. Idczak, P. Mazur, L. Markowski, M. Skiścim, and M. Musiał. *Applied Surface Science*, **2012**, 258, 21, 8349–8353.
55. B. Zhang, T. Kong, W. Xu, R. Su, Y. Gao, and G. Cheng. *Langmuir*, **2010**, 26, 6, 4514–4522.
56. A. Viinikanoja, J. Lukkari, T. Ääritalo, T. Laiho, and J. Kankare. *Langmuir*, **2003**, 19, 7, 2768–2775.
57. V. Zoulalian, S. Zürcher, S. Tosatti, M. Textor, S. Monge, and J. J. Robin. *Langmuir*, **2010**, 26, 1, 74–82.
58. D. R. Wheeler and O. D. Faut. *Appl. Surf. Sci.*, **1984**, 18, 1–2, 106–122.
59. M. F. Beaux, N. J. Bridges, M. Dehart, T. E. Bitterwolf, and D. N. McIlroy. *Appl. Surf. Sci.*, **2011**, 257, 13, 5766–5771.
60. M. (1980). Brückner, R., Chun, H.-U., Goretzki, H., Sammet. *Journal of Non-Crystalline Solids*, **1980**, 42, 49–60.
61. [J. Stypula, B., Stoch. *Corros. Sci.*, **1994**, 36, 12, 2159–2167.
62. [C. D. Wagner, W. M. Riggs, L. E. Davis, and J. F. Moulder, *Handbook of X-Ray Photoelectron Spectroscopy*. **1979**.
63. H. S. O. Chan, T. S. A. Hof, K. L. Tan, and L. Ying-Phooi. *Inorganica Chim. Acta*, **1991**, 184, 1, 23–26.
64. D. H. Yang, Q. J. Xue, X. S. Zhang, H. Q. Wang, W. L. Lin, and X. J. Ding. *Wear*, **1994**, 173, 1–2, 129–135.

65. L. S. Dake, D. R. Baer, D. M. Friedrich, L. S. Dake, D. R. Baer, and D. M. Friedrich. *J. Vac. Sci. Technol. A*, 2014, 1634, **1989**.
66. P. Lo, W. Tsai, J. Lee, and M. Hung. *Surf. Coatings Technol.*, **1994**, 67, 1, 27–34.
67. I. M. Watson, J. A. Connor, R. Whyman, and T. Heath. *Thin Solid Films*, **1991**, 201, 337–349.
68. J. P. Delville, E. Hugonnot, C. Labrugère, T. Cohen-Bouhacina, and M. H. Delville. *J. Phys. Chem. C*, **2010**, 114, 46, 19782–19791.
69. Y. Liu, H. Lin, and C. Mou. *Langmuir*, **2004**, 20, 8, 3231–3239.
70. K. H. Nam and L. L. Tavlarides, *Chem. Mater.*, **2005**, 17, 6, 1597–1604.
71. D. Das, M. K. Sureshkumar, K. Radhakrishnan, J. Nuwar, and C. G. S. Pillai. *J. Radioanal. Nucl. Chem.*, **2011**, 289, 1, 275.
72. Y.-S. Yun, D. Park, J. M. Park, and B. Volesky. *Environ. Sci. Technol.*, **2001**, 35, 21, 4353–4358.
73. T. Cordero, J. Rodriguez-Mirasol, N. Tancredi, J. Piriz, G. Vivo, and J. J. Rodriguez. *Ind. Eng. Chem. Res.*, **2002**, 41, 24, 6042–6048.
74. M. A.S.D. Barros, E.A. Silva, P.A. Arroyo, C.R.G. Tavares, R.M. Schneider, M. Suszek, E.F. Sousa-Aguiar. *Chem Eng Sci.* **2004**, 59 5959 – 5966.
75. Y-G. Chen, Yong He, Wei-Min Ye, Ling-Yan Jia. *J. Ind Eng Chem.* 26 (**2015**) 335–339.
76. Dybowski, C.; Bai, S. *Anal. Chem.* **2000**, 72, 1R-7R
77. Eichele, K.; Ossenkamp, G. C.; Wasylshen, R.E.; Cameron, T. S. *Inorg. Chem.* **1999**, 38, 639-651.
78. Olivieri, A.C. *Solid State Nuclear Magnetic Resonance* (**1997**), 10, 19-24.
79. Kempermann, H.; Bain, A. D.; Dumont R.S. *J. Chem. Phys.* (**2002**), 116, 2464-2471.
80. Bemis, L.; Clark, H. C.; Davies, J. A.; Fyfe, C. A.; Wasylshen, R. E. *J. Am. Chem. Soc.* **1982**, 104, 438-445.